DOI: 10.37190/ ABB-02339-2023-02

Bioactive glasses enriched with zinc and strontium: synthesis, characterization, cytocompatibility with osteoblasts and antibacterial properties

Lidia Ciołek[1*], Milena Chraniuk[2], Piotr Bollin[2], Monika Biernat[1], Mirosława Panasiuk[2], Dawid Nidzworski[2], Beata Gromadzka[2], Zbigniew Jaegermann[1], Elżbieta Pamuła[3]

[1] Biomaterials Research Group, Ceramic and Concrete Division in Warsaw, Lukasiewicz Research Network – Institute of Ceramic and Building Materials, Cracow, Poland

[2] Department of *in vitro* studies, Institute of Biotechnology and Molecular Medicine, Gdansk, Poland

[3] Department of Biomaterials and Composites, Faculty of Materials Science and Ceramics, AGH University of Science and Technology, Cracow, 30-059, Poland

*Corresponding author: Lidia Ciołek, Biomaterials Research Group, Ceramic and Concrete Division in Warsaw, Lukasiewicz Research Network – Institute of Ceramic and Building Materials, Cracow, Poland, e-mail address: lidia.ciolek@icimb.lukasiewicz.gov.pl

Submitted: 6th November 2023

Accepted: 7th February 2024

Abstract

Purpose: The aim of the presented work was to characterize the new obtained bioglasses and assess their biological performance *in vitro*. Bioglasses were produced using the sol-gel method in the SiO_2-P_2O_5-CaO system, for the purpose as composite ingredients. Their chemical composition was enriched with ZnO to introduce antibacterial properties and SrO with osteoinductive effect. The properties of bioglasses were compared and the effect of chemical composition and particle size on their biological properties was assessed. **Methods:** The bioglasses were evaluated via TG-DTA, FTIR, SEM-EDS analyses before and after incubation in SBF solution. LDH and WST-1 tests were used to determine the level of cytotoxicity of the tested bioglasses on hFOB1.19 osteoblasts. **Results:** The results show that the developed bioglasses release Ca^{2+}, are bioactive in SBF solution, not cytotoxic and show antibacterial activity in contact with *Pseudomonas aeruginosa* and *Staphylococcus aureus* strains. Bioglasses enriched with ZnO show the highest bactericidal activity. All tested bioglasses enhanced hFOB 1.19 cells proliferation. Particle size has a lower effect on biological performance of the bioglasses than their chemical composition. **Conclusions:** The conducted research showed that bioglass modification with SrO and ZnO can be considered particularly for the development of biomaterials supporting bone regeneration and the treatment of infected bone defects.

Key words: bioglass, bioactivity, cytotoxicity, antibacterial activity

1. Introduction

The field of biomaterials is constantly evolving and searching for innovative solutions. Future bioactive materials, including bioglasses, are expected to contain required physical features such as the appropriate morphology, porosity, and specific chemical structure allowing release of active molecules promoting bone remodelling and controlled biodegradation of the implant [7]. The rate of degradation of the composite is also affected by the size of the bioactive glass grains, the greater the number and the smaller the size of the glass particles, the faster the mass loss. Integration of bone tissue with the implant as well as prevention and treatment of bacterial infections still remain a major challenge. To achieve the desirable properties of biomaterials, researchers and clinical investigators are still working on new solutions. In the literature, much attention is paid to the bioactivity of materials [10] and factors inducing osseointegration – thanks to which bone cells are stimulated to create a direct connection with the implant [12]. Osseointegration is a multi-stage process, consisting of many reactions that leads to a permanent

connection of the implant with the bone tissue. In addition, it is becoming increasingly difficult to treat bacterial infections due to the emergence of antibiotic-resistant bacteria. The prevention of bacterial infections by incorporating the components that possess antibacterial activity into the new biomaterials is often described [19]. In conducted research, much attention is paid on bioactive glasses [6,39,22] and natural polymers from which biocomposites are made [31]. Bioglass and glass-ceramic materials are widely used to directly fill or replace bone lesions. Oftentimes, they are also used as a component of multifunctional composites in biomaterial engineering [10,39,31]. The use of the sol-gel method in the production of bioglasses provides them many beneficial functional properties [10]. One of them is high bioactivity, i.e., the ability to create a hydroxyapatite intermediate layer at the material/bone tissue interface. Nucleation of apatite crystals occurs by chemisorption of calcium and phosphate ions to the silicic acid gel layer, easily formed on the bioglass surface. The reactions at the interface of the bioglass and bone tissue during the process of apatite formation in three-component SiO_2-P_2O_5-CaO system follow the scheme presented by L. Hench [13]. The growth of apatite crystals occurs mainly thanks to calcium ions released from the bioglass, which react with inorganic phosphate groups present in body fluids circulating in the bone microenvironment. This process leads to the formation of a hydroxyapatite layer and its connection with the collagen fibers of the organic matrix. As demonstrated by others, the ions released in certain concentrations from the biomaterial play an important role in the bone regeneration process. Ions released from the biomaterial generate a favorable microenvironment that facilitates cell proliferation. In the process of stimulating new bone growth, the synergistic effect of ions released from the bioglass or biomaterial, i.e., silicon and strontium, is also important [23]. Modification of the composition of bioglass by partially replacing Ca^{2+}in the glass network with Mg^{2+} or Sr^{2+} increases the surface reactivity, which in turn enhances the ability to form hydroxyapatite deposits during contact with body fluid.

Strontium is clinically used as a pharmaceutical agent for osteoporosis treatment because of its ability to activate osteoblasts and inhibit osteoclast activity [14]. Strontium ions released from modified bioglass have an osteoinductive effect by improving the proliferation of osteoblasts, and also have antibacterial properties [1]. The results presented by Gorustovich et al. [11] confirm the positive effect of strontium ion the process of osteogenesis. Replacing CaO by SrO is regarded as a novel biomaterial formation strategy for use in bone repair and regeneration therapy.

Additionally to strontium, zinc is one of the important components present in bones, which shows the stimulatory effect on the bone mineral deposition process, in both *in vitro* as well as

in vivo conditions. Zinc homeostasis is essential to many proteins which regulate cellular functions such as the response to oxidative stress, DNA replication, DNA damage repair and apoptosis [37]. Zinc ions are components or activators of many enzymes involved in metabolic processes [3] and was shown to stimulate the early differentiation of bone cells [36]. Taking into account these characteristics of zinc, many studies focus on the use of zinc as a component of bioactive glasses or other biomaterial types [2]. As shown by Vukomanovic et al. [35], zinc ions released from bioactive glasses containing ZnO stimulate the proliferation and osteogenic differentiation of cells and facilitate the development of a mature bone. Moreover, zinc ions also increase bone density, have anti-inflammatory and antibacterial properties, and thus facilitate bone healing. The presence of ZnO in the glass enhances its mechanical strength and chemical durability and reduces its degradability in aqueous media such as simulated body fluid (SBF) [17]. According to literature data, the amount of released zinc ions from the biomaterial should be optimal, i.e., safe for the treated patient, and able to ensure a minimum inhibitory or bactericidal concentration [19,28]. The dominant hypothesis of the mechanism of bacterial destruction by ZnO-containing biomaterials is the formation of reactive oxygen species (ROS) and the destruction of the cell wall after contact with ions or labile zinc complexes [32].

Bioactivity and cytotoxicity of bioglasses can be tested with the use of various methods [29]. Additionally, many published papers which describe direct contact of cells with glass particles, use small amounts of bioglass [40] or do not include weights of samples [24]. This could lead to the conclusion that the total mass of bioglass used in the experiment was insufficient to properly assess the influence of bioglass on their biological performance. On the other hand, increased amount of bioglass in direct contact with cells may cause mechanical damages of *in vitro* model. This problem highlights the importance of developing new methodologies that will allow for the use of higher bioglass mass per test, eliminate direct particle contact with cells, and maintain continuous ion release throughout the experiment which is not possible in research based on bioglass extracts.

The purpose of this study was to synthesize and characterize the newly obtained bioactive glasses, as well as to evaluate their bactericidal properties and *in vitro* cytocompatibility with osteoblasts. New methodology in cell-based assays was used due to the limitations of the previously described bioglass cytotoxicity testing protocols. The improved methodology was based on cellular growth in the presence of increased mass of biolglass placed in cell culture inserts which allowed for ion release to be maintained throughout the experiment and assessed for its influence on osteoblasts. The obtained results will be valuable due to the possibility of

the use of selected bioglasses as components for innovative multifunctional composites for filling bone tissue defects.

2. Materials

In order to obtain bioglass, the following components were used: tetraethoxysilane, zinc nitrate (V) hexahydrate, calcium nitrate (V) tetrahydrate (Avantor Performance Materials Poland S.A., Gliwice, Poland), strontium nitrate (V) (Sigma-Aldrich, St. Louis, MO), and triethyl phosphate (V) (Fluka, Chemie GmbH, Buchs, Switzerland).

Formation of sol-gel derived bioglass

Five chemical compositions of bioglass have been developed in the SiO_2-P_2O_5-CaO system. Bioglass with SiO_2 content of 70 wt.%, P_2O_5 content of 5 wt.% and CaO content of 25 wt.% constituted the reference material (sample P5). In compositions of bioglass supplemented with SrO or ZnO, 2 wt.% or 5 wt.% CaO was replaced with SrO or ZnO (samples P5Sr2, P5Zn2, P5Sr5 and P5Zn5, respectively). The low-temperature sol-gel method was used to produce these bioglasses. The beaker with the reaction mixture was placed in an dryer and kept for 7 days at 40°C. After each subsequent 7 days, the drying temperature was increased to 60°C, 80°C, 120°C and 180°C, respectively. After holding for 7 days at 180°C, the dried gel was transferred to a ceramic crucible and placed in an electric furnace. After the drying was completed, the dry gel was heated in an electric furnace. For the TG/DTA test, a sample of P5 bioglass was prepared by annealing at 600°C for 10 h. After the test, all glasses were heated at 650°C for 15 h to stabilize their structure. Five bioglasses were obtained: P5, P5Sr2, P5Zn2, P5Sr5 and P5Zn5 in the form of coarse-grained powders. Next, the powders were crushed in a mechanical mortar for 15 min and subjected to grinding in a rotary-vibrating mill. Each of the glasses was prepared in two groups differing in grain size. The grinding time in the rotary-vibration mill was 10 minutes for group I and 20 minutes for group II. Ten bioglasses in the form of powders were obtained in this way, marked with the symbols: P5_I, P5_II, P5Sr2_I, P5Sr2_II, P5Zn2_I, P5Zn2_II, P5Sr5_I, P5Sr5_II, P5Zn5_I and P5Zn5_II.

3. Methods

Low angle laser light scattering – particle size analysis

The analysis was performed using a Malvern Instruments 2000 laser particle size analyzer using the low-angle laser light scattering (LALLS) method. The LALLS allowed for evaluation of the particle size in a wide range from 0.1 μm to 2000 μm with a margin error of 0.5%. The obtained characteristic values were dv(0.1) – meaning that the size of 10% vol. particles of the sample population is smaller than the dv value, dv(0.5) – meaning that the size of 50% vol.

particles of the sample population is smaller than the dv value, dv(0.9) – meaning that the size of 90% vol. particles of the sample population is smaller than the dv value.

Thermogravimetric Analysis (TG) / Differential thermal analysis (DTA) – study of physicochemical changes occurring during heating

DTA/TG analysis was performed using the STA 449 F3 Jupiter® NETZSCH device for simultaneous thermal analysis (TG, DTA/TG, DSC/TG). 4.9 mg of bioglass was placed in a 0.3 ml alumina DTA crucible. The analysis was carried out in the temperature range 30–1000°C, with the temperature change rate 10°C/min, in an argon atmosphere (70 ml/min). A separate corrective measurement of the empty crucible was also carried out.

Fourier Transform Infrared (FTIR) Spectroscopy – identification of functional groups in glasses

FTIR-ATR analysis was performed using the FTIR TENSOR Bruker spectrophotometer equipped with a DLaTGS detector. To prepare the samples (tablets with KBr), 1.5 mg of bioglass sample per 200 mg of dried KBr was used. The samples were tested in the transmission mode with the following instrumental settings: wavenumber range 400−4000 cm^{-1}, number of scans 64, spectral resolution 4 cm^{-1}. Each sample was measured twice to check structural reproducibility. The baseline correction and atmospheric compensation procedure has been applied to the presented spectra with Opus 7.2 software.

Estimation of the amount of calcium ions released into deionized water

From each type of bioglass, 0.3 g of powder with particle size I was weighed and transferred to a glass vessel, filled with 150 ml of deionized water with conductivity of 0.05 μS/cm and sealed. The dishes were kept in an incubator at a constant temperature of (37±1)°C for 21 days. Samples for testing the amount of released calcium ions were collected after 1 h, 24 h, 7 days and 21 days. The concentration of released Ca^{2+} ions was determined using flame atomic absorption spectrometry (FAAS) . The stock solution was prepared using Merck KGaA's Titrisol (1000 mg Ca, $CaCl_2$ in 6.5%wt. HCl). Standard solutions were prepared by the method of successive dilutions. Each measurement was performed in triplicate.

Evaluation of bioactivity by means of SEM-EDS analysis

The microstructure of the glasses was examined by scanning electron microscopy (SEM) with energy dispersion spectroscopy (EDS). Micro-area analysis was performed before and after incubation in simulated body fluid (SBF) to determine the bioactivity of the produced bioglasses.. Ion concentrations in the SBF solution in $mmol/dm^3$ were: Na^+ 142; K^+ 5,0; Mg^{2+}

1,5; Ca^{2+} 2,5; Cl^{-} 148,8; HCO_3^{-} 4,2; HPO_4^{2-} 1,0 and SO_4^{2-} 0,5. Bioglasses were prepared in the form of discs with a diameter of 6 mm and a height of 2 mm on a single-axis press with a pressure of 5 kN. Six discs of each material were placed in sealed glass vessel and 65 ml of the SBF solution were introduced. The sample vessels were incubated at 37±1°C for up to 4 weeks. The initial pH of the SBF solution was 7.25. After 7, 14 and 28 days of incubation, samples were collected and changes in surface morphology were assessed and their qualitative chemical composition by EDS was determined.

Cytotoxicity testing

Cells

Human foetal osteoblasts hFOB 1.19 (ATCC CRL-11372, USA) were cultured in a 1:1 mixture of Ham's F12 medium and Dulbecco's modified Eagle's medium with 2.5 mM L-glutamine (without phenol red). The medium was supplemented with 10 µg/ml gentamicin and 0.25 µg/ml amphotericin B and foetal bovine serum (FBS) at a final concentration of 10%. Cells were cultured at 34°C and 5% CO_2.

Bioglasses testing via cell culture inserts

Human osteoblast hFOB cells were plated in 12-well plates at 3×10^5 cells/well in 800 µl of cell medium. Next, 0.1 g of bioglasses enriched with zinc and strontium oxides has been weighed on cell culture inserts (Sarstedt, Germany) and placed into wells. Additional 400 µl of medium was added to each insert. Cells were incubated for 48 h at 37°C, 95% humidity, 5% CO_2. Cell proliferation and cytotoxicity were determined by WST-1 and LDH tests, respectively.

Cytotoxicity – Lactate Dehydrogenase (LDH) activity assay

The test was performed using the Cytotoxicity detection kit (Roche Applied Science, Germany) according to the supplier's protocol. Briefly, the dye solution was mixed with the catalyst solution and added to the samples previously transferred to 96-well plates. After incubation in the dark, the optical density of the samples at 490 nm and 690 nm was measured using a plate reader Epoch (BioTek Instruments, USA). As a positive control, cells treated with 1% Triton - X100 were used. Untreated cells and a blank medium were included into each assay.

The cytotoxicity percentage was calculated as follows:

Cytotoxicity = (Sample absorbance - Control absorbance)/(Positive control absorbance - Control absorbance) x 100%.

WST-1 mitochondrial activity assay

For WST-1 assay hFOB 1.19 cells were incubated with bioglasses enriched with zinc and strontium oxides placed on cell culture inserts (Sarstedt, Germany). Cells with inserts

containing bioglass were incubated for 48 h at 37°C, 95% humidity, 5% CO_2. The proliferation of hFOB 1.19 cells was determined using the WST-1 assay kit (Abcam, USA) according to the supplier's protocol. Briefly, the cells were incubated with the extract and then treated with 40 µl of the WST-1 reagent followed by 2 h incubation in 34°C and 5% CO_2. Conditioned medium was collected from each well and transferred to a 96-well flat bottom plate (Sarstedt, Germany). The optical density at 450 nm and 620 nm was measured using an Epoch plate reader (BioTek Instruments, USA). Untreated cells and a blank medium were included into each assay. The proliferation percentage was calculated as follows:

Proliferation = (Sample absorbance / Control absorbance) x100%

Antibacterial activity of bioglasses

Preparation of bacterial cultures

Two bacterial reference strains were chosen: *Staphylococcus aureus* PCM 2602 and *Pseudomonas aeruginosa* PCM 2563. Both selected pathogens are of high clinical importance [25]. All bacteria were grown overnight at 37°C in Lysogeny Broth (LB, BTL, Poland). Prior to the experiments, the cultures were diluted to reach a cell density of 0.5 McF (McFarland standard) corresponding to approximately $1.5x10^8$ cells/ml. LB medium consisted of 10 g/l casein peptone, 5 g/l yeast extract and 10 g/l NaCl with a final pH of 7.0.

Determining the antibacterial activity of bioglass

The antibacterial activity of bioglass was analysed in a manner similar to that presented by Hu et al. [15]. In the experiments, 100 mg of each biomaterial was added into 1 ml of bacterial suspension in separate Eppendorf tubes. Also, samples consisting of 100 mg of SiO_2 particles or gentamicin at a final concentration of 100 µg/ml in 1 ml of bacterial suspension were tested. Bacterial suspensions without any additive served as a control. After 1 min of stirring with a vortex mixer, Eppendorf tubes with samples were placed in aerobic conditions at 37°C for 1 h. After the incubation, serial dilutions of the suspensions were made, followed by spreading the volume of 100 µl on LB-agar plates. The number of resultant colonies were counted as CFU/ml (colony forming units) after 24 h of incubation at 37°C. The number of viable microorganisms and the percentage of bacterial count reduction were calculated in relation to the bacterial colonies number from control. All experiments were performed in triplicates.

Statistical analysis

GraphPad Prism (GraphPad Software, USA) was utilized for data analysis and visualization. The statistical analysis was conducted using the Kruskal–Wallis test. Next, the Benjamini, Krieger, and Yekutieli multiple comparison test ($p< 0.05$) was conducted to control the false

discovery rate. The repetition number of bioglass sample in one experiment was n ≥ 4 for cytotoxicity and WST-1 mitochondrial activity assay. P< 0.05 were considered significant.

4. Results

Particle size analysis

The particle size distribution of the obtained bioglasses was described using the characteristic values determined using the LALLS method. The characteristic sizes dv(0.1), dv(0.5) and dv(0.9) of the particles of the obtained bioglasses: P5_I, P5_II, P5Sr2_I, P5Sr2_II, P5Zn2_I, P5Zn2_II, P5Sr5_I, P5Sr5_II, P5Zn5_I and P5Zn5_II are shown in Table 1.

It can be observed that for bioglasses with particle size I, the values of the dv(0.5) dimension ranged from 45.5 μm for the P5Zn2_I sample to 69.1 μm for the P5Sr2_I sample. On the other hand, for bioglasses with particle size II, the values of dv(0.5) were lower and ranged from 26.8 μm for the P5_II sample to 45.0 μm for the P5Sr2_II sample.

Table 1: The particle size results obtained using the LALLS method.

Symbol of bioglass	Particle size, μm		
	dv(0.1)	dv(0.5)	dv(0.9)
P5_I	7.1	59.9	215.5
P5_II	4.2	26.9	77.4
P5Zn2_I	5.4	45.5	139.5
P5Zn2_II	3.7	29.1	85.6
P5Sr2_I	8.3	69.1	228.6
P5Sr2_II	5.7	45.0	131.1
P5Zn5_I	8.0	68.1	198.5
P5Zn5_II	5.4	42.3	118.7
P5Sr5_I	7.7	61.8	173.7
P5Sr5_II	4.9	37.7	106.0

The obtained powders differed in particle size parameters both in group I and II, despite the fact that the grinding times of particular bioglasses were always the same. The differences in the particle size parameters result mainly from the grinding method used and the differences in the microstructure of the glasses.

Thermogravimetric Analysis TG / Differential thermal analysis (DTA)

The results of thermogravimetric and differential thermal analysis obtained for P5 bioglass annealed at 600°C for 10 h are shown in (Figure 1). The changes visible on the TG curve correspond to the thermal processes reflected in the DTA curve. During the heating of the sample from room temperature to 425°C, the weight loss on the TG curve was 12.3 wt.%.

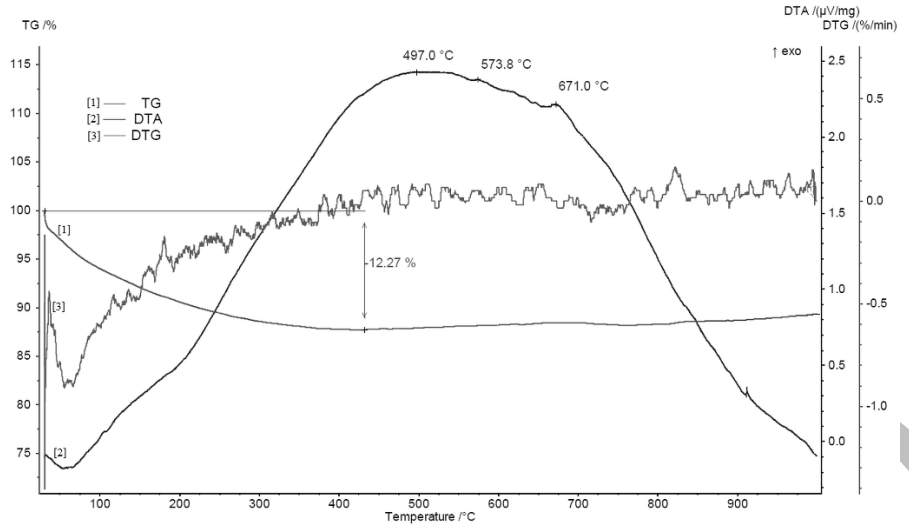

Figure 1: TG/DTA analysis of bioglass P5_II annealed 10 h at 600°C.

A small peak on the DTA curve in the range of 50–180°C for our bioglass, which was previously annealed at 600°C, is related to the loss of moisture adsorbed in its pores. On the other hand, in the temperature range of 425–700°C, a broad DTA signal was observed. Several signals of lower intensity can be distinguished in the DTA curve: 497.0°C, 573.8°C, 671.0°C.

The performed thermal analysis helped to determine the temperature of the thermal treatment (650°C) necessary to stabilize the microstructure of the produced bioglasses.

FTIR

The FTIR spectra of bioglasses P5, P5Sr2, P5Sr5, P5Zn2, and P5Zn5 annealed 15 h at 650°C in particle size II are shown in Figure 2. FTIR analysis was performed to identify the main functional groups and study the effect of different chemical compositions of the synthesized bioglasses particles on the chemical structure. For all of the bioglasses, the main absorption bands appeared at 1070 and 798 cm^{-1} and correspond to the stretching vibrations of $[SiO_4]^{4-}$ tetrahedra. The wide absorption bands at 1220 and 1070 cm^{-1} are associated to asymmetric stretching vibrations of Si-O-Si and bands at 798 cm^{-1} are assigned to symmetric stretching vibration of Si-O-Si (combining of tetrahedra $[SiO_4]^{4-}$). Low-intensity dual peaks of P-O asymmetric bending vibrations of PO_4^{3-} groups were identified at 565 and 582 cm^{-1}. The broad bands observed at 460 cm^{-1} are attributed to the bending vibration of Si-O-Si. The spectra also show weak bands at 1636 cm^{-1} attributed to the bending vibration of HOH. Wide, medium-intensity bands in the range of 3100-3700 cm^{-1} from the stretching vibrations of OH bonds in silanol groups (Si-OH) and HO-H bonds in adsorbed water molecules were also observed.

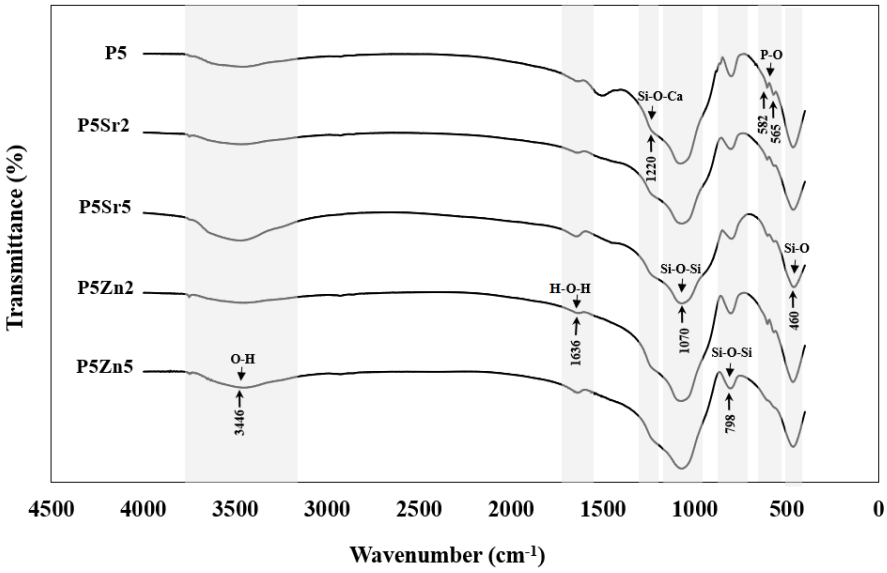

Figure 2: FTIR analysis of bioglass P5_II, P5Sr2_II, P5Sr5_II, P5Zn2_II and P5Zn5_II.

Assessment of the concentration of Ca^{2+} ions released into deionized water

The result of the analysis carried out using optical emission spectrometry with inductively coupled plasma (ICP-OES) confirms the release of Ca^{2+} ions (Figure 3) and indicates the activity of the tested bioglasses.

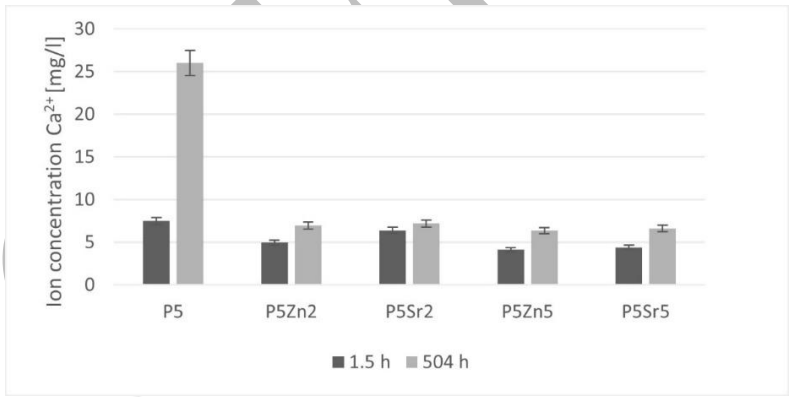

Figure 3: The concentration of released Ca^{2+} ions to deionized water after the degradation of glasses: P5_I, P5Zn2_I, P5Sr2_I, P5Zn5_I and P5Sr5_I. The total measurement uncertainty was determined with a confidence level of 95% and a coverage factor of k=2.

For glasses P5Zn2_I, P5Sr2_I, P5Zn5_I and P5Sr5_I, the concentration of determined ions after contact with deionized water for 504 h (21 days) was only slightly higher than those determined after 1.5 h. A significantly higher amount of released ions after 21 days was observed only for P5_I glass.

Evaluation of bioactivity in SBF solution

An assessment of bioactivity was carried out on the basis of SEM-EDS analyses of bioglasses before and after incubation in SBF solution. This method of assessing bioactivity is used by

other researchers [21]. The results of the analysis of bioglasses before incubation are shown based on the example of P5_II bioglass heated at 650°C. The SEM image of this bioglass before incubation in SBF with EDS analysis is shown in (Figure 4).

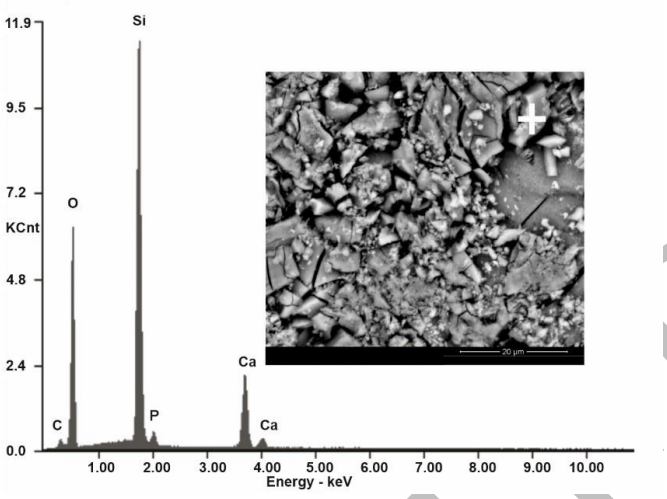

Figure 4: SEM-EDS analysis of bioglass P5_II before incubation in SBF.

The SEM-EDS analysis shows an increase in the intensity of the Ca and P peaks and a significant decrease in the Si peak.

A high Si peak and lower Ca and P peaks were observed in the EDS diffraction spectrum. A similar dependence of the intensity of the peaks was also observed for the remaining bioglasses (SEM images and EDS spectra not shown in the manuscript). The EDS analysis for the remaining bioglasses under consideration confirms the presence of Si, Ca and P in the composition of the P5, and additionally the presence of Zn or Sr in bioglass enriched with ZnO or SrO, respectively. In the images taken after 2 weeks of incubation in the SBF solution, clearly visible spherical forms and changes in chemical composition were observed on the surface of all the tested bioglasses (Figure 5).

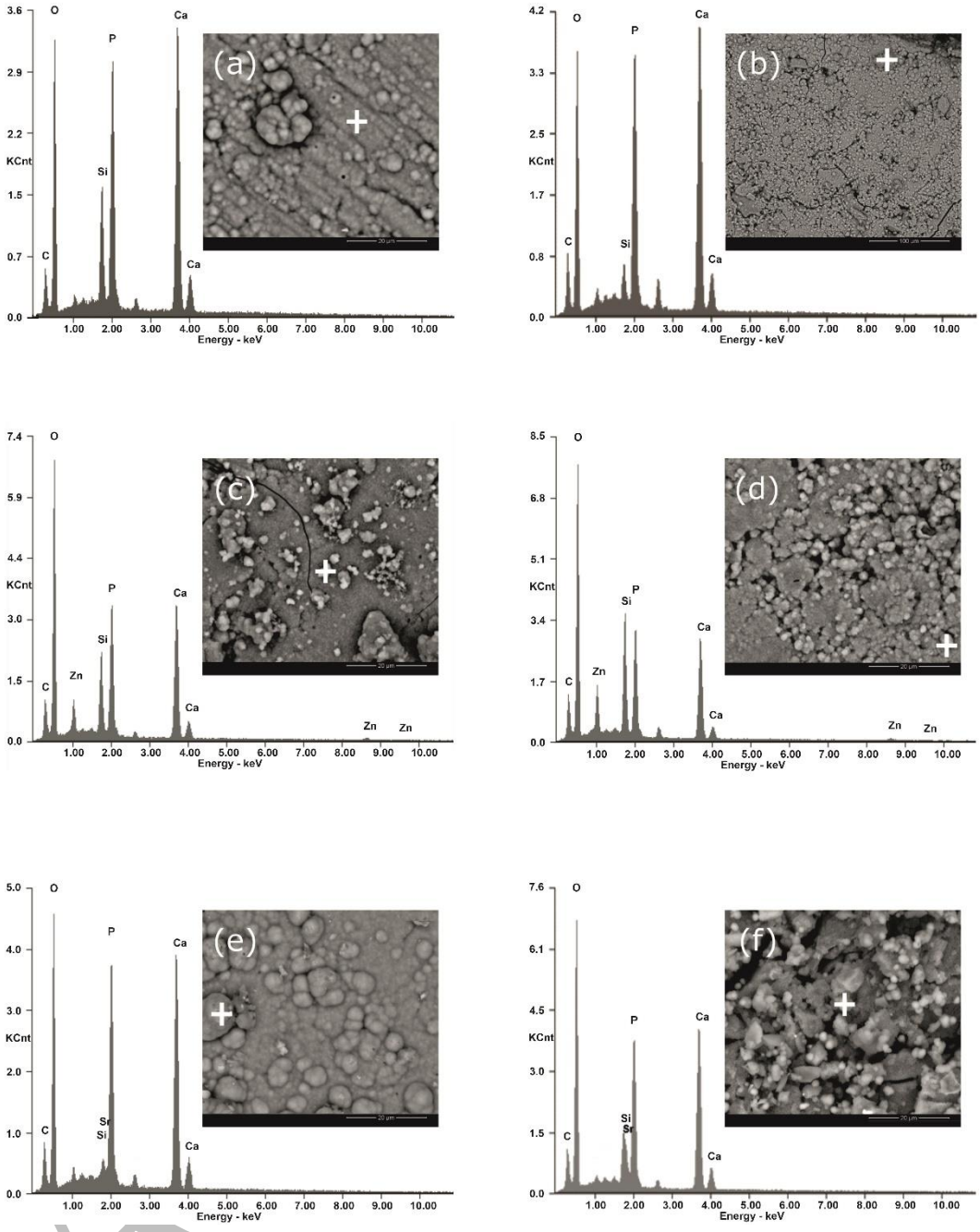

Figure 5: SEM-EDS analysis of glasses (a) P5_II/600, (b) P5_II/650, (c) P5Zn2_II/650, (d) P5Zn5_II/650, (e) P5Sr2_II/650, (f) P5Sr5_II/650 after 14 days incubation in SBF.

Biological evaluation of bioglasses

Cytotoxicity testing

LDH and WST-1 tests were used to determine the level of cytotoxicity of the tested bioglasses towards the hFOB1.19 cells. The test procedure and evaluation of the results were carried out in accordance with the EN ISO 10993-5:2009 standard "Biological evaluation of medical devices – Part 5: In vitro cytotoxicity tests." Due to the fact that hFOB1.19 osteoblasts divide

every 36 h, the tests were performed after 48 h of incubation. The cytotoxicity results obtained are presented in (Figure 6).

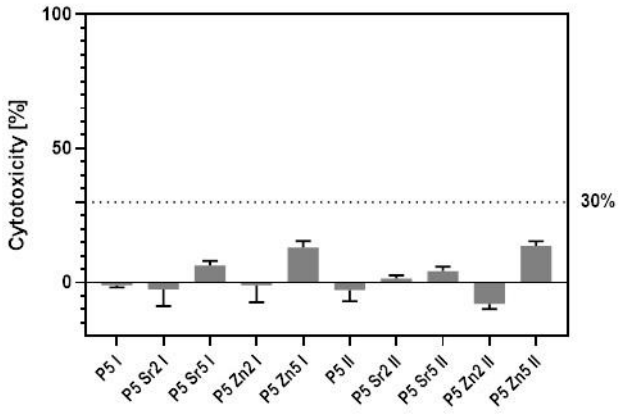

Figure 6: Cytotoxicity of bioglasses measured in LDH test after 48 h of incubation with tested bioglasses.

Leakage of lactate dehydrogenase form osteoblasts incubated with the test glasses did not exceed 30% of control for any of tested samples. This allows to classify the tested bioglasses as a material that does not cause cytotoxic effect. The highest average cytotoxicity value was recorded for bioglass samples containing 5% ZnO, it was 13.0 ± 2.5% and 13.6 ± 1.8% for P5Zn5 I and P5Zn5 II, respectively. The obtained results indicate that the chemical composition has a greater influence on the cytotoxicity of the tested bioglasses than the particle size.

The statistical analysis of cytotoxicity test results revealed activity differences between P5 Zn2 II and the following bioglasses: P5 Sr5 I, P5 Sr5 II, P5 Zn5 I, and P5 Zn5 II. Cytotoxicity results for P5 Sr2 II bioglass were statistically different in comparison to P5 Zn2 II, P5 Zn5 I, and P5 Zn5 II. Next, statistically significant differences were identified between P5 II and P5 Sr5 I, P5 Zn5 I, and P5 Zn5 II. Statistically significant differences in cytotoxicity test were detected also for P5 Sr2 I and effects caused by P5 Sr5 I, P5 Zn5 I, and P5 Zn5 II. P5 I and P5II bioglasses caused statistically different effects in comparison to P5 Zn5 I and P5 Zn5 II. Despite discovered differences, it is essential to remember that all cytotoxicity results allowed to classify bioglasses as nontoxic.

The results of the WST-1 assay used to evaluate the proliferation of hFOB1.19 cells are shown in (Figure 7). The results of proliferation of all tested bioglasses exceeded the threshold of 70%. The highest proliferation among the bioglass with particle size I was determined for samples P5_I. On the other hand, among the bioglass with particle size II, the highest proliferation was determined for P5Sr2_II and P5Zn2_II samples.

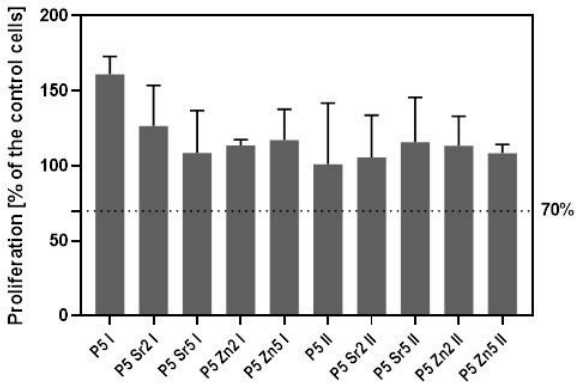

Figure 7: Proliferation of osteoblasts incubated 48 h with tested bioglasses.

Antibacterial activity of bioglasses

The antibacterial activity test of the examined bioglasses was carried out in the presence of gentamicin as a positive control and SiO_2 as a negative one. The results of the test indicate a decrease in the number of bacteria of both species for all tested bioglasses (Figure 8).

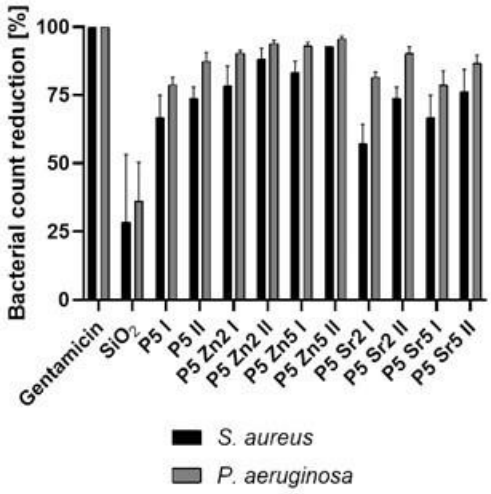

Figure 8: Bacterial count reduction of *S. aureus* and *P. aeruginosa* incubated with bioglasses and gentamycin as control.

The observed results of bacteria cell reduction number by the tested bioglasses, regardless of the particle size, are lower than for gentamicin, but much higher than for negative control. SiO_2 reduced the initial number of both analyzed bacteria species by an average of 32%. In the case of *P. aeruginosa*, the reduction in the number of microorganisms for eight tested bioglasses exceeded 80%. The value of reduction in relation to the initial number of microorganisms for P5Zn2 II and P5Zn5 II bioglasses was 93.9% and 95.6%, respectively. In the case of *S. aureus*, the highest reduction values were also determined for the P5Zn2 II and P5Zn5 II samples and they were 88.1% and 92.9%, respectively. Bioglasses containing ZnO showed a higher

reduction value than the reference bioglass P5 and bioglasses containing SrO. The determined percentage of bacterial count reduction for P5Sr2 I and P5Sr5 II bioglasses was lower than for P5 I and P5 II glasses by 9.5 and 0.7%, respectively. In addition, bioglasses with a finer particle size were characterized by higher reduction efficiency, on average by 13.2% against *S. aureus* and 7.0% against *P. aeruginosa*.

5. Discussion

It was observed that the determined weight loss was similar to that reported in the literature for the stabilized gel [28]. According to the literature, during wet gel analysis, changes in mass in the range of 50–120°C are related to the loss of moisture and the endothermic transformation characteristic of the volatilization of water and ethanol residues. During heating dry gel above 120°C, exothermic transformations occur, related to the condensation process as well as thermal decomposition of nitrates and removal of NO_2. The weight loss related to the thermal changes taking place for the wet gel is 60 wt.% and for dry gel exceeds 30 wt.% [30]. The obtained results of ion release may indicate that the particle size has a smaller impact on hydrolytic activity than the microstructure of bioglass. According to the results presented by Vaid et al. [34], the release of ions also leads to other chemical transformations, especially during the incubation of bioglasses in the SBF solution. During the contact of bioglasses with the SBF solution, due to the released Ca^{2+} ions, amorphous calcium phosphate is formed over a hydrated layer rich in silicon, crystalline calcium phosphate or apatite. On the other hand, the results of Liu et al. research [20] indicate that the increase in the content of calcium ions in the SBF solution is not a critical factor influencing the precipitation of apatite. The observed changes in the SEM-EDS analysis are consistent with the results reported by other researchers. Changes occurring on the surface of bioglasses during contact with SBF result from a number of phenomena including leaching, dissolution and precipitation, which lead to the formation of an apatite layer [13] or a calcite layer. It is believed that the appearance of apatite on the biomaterial surface similar to HA nanocrystals found in human bones promotes cell adhesion and proliferation. In addition, the replacement of Ca by Sr in the chemical composition of the glass promotes bone formation. According to Fredholm [8], the presence of SrO promotes the release of ions and the formation of apatite. The beneficial effect of Sr on cell adhesion and proliferation [27] and on differentiation [16,33] was demonstrated in the literature. The influence of bivalent ions in the chemical composition, i.e., Zn^{2+} and Sr^{2+}, on the biological properties of bioglass was described by Cacciotti et al. [4]. The authors demonstrated that ionic dissolution products of bioglass are able to induce and stimulate the expressions of genes related

to the osteoblastic differentiation and bone formation. The studies [9] show that Sr can promote osteoblast activity and inhibit osteoclasts *in vitro*. Also Murphy et al. showed that the appropriate concentration of released Sr^{2+} can induce a positive response of osteoblastic phenotype cells [26]. Kargozar, in *in vivo* studies, found that they promote both osteogenesis and angiogenesis [18]. In our studies, bioglass containing strontium in the chemical composition did not showed increased proliferation compared to glasses enriched with zinc. The obtained bacterial count reduction results also indicate a higher sensitivity of *P. aeruginosa* bacteria compared to *S. aureus* to bactericidal agents present in contact with the tested bioglasses and SiO_2. The obtained results also show the influence of differences in the structure of the cell wall between Gram-negative and Gram-positive bacteria and the sensitivity of the species to the antibacterial agent [28], as well as the chemical composition and particle size of the analyzed material. According to Pasquet et al [28], the concentration of Zn^{2+} plays a significant role, because in order to obtain a similar antibacterial effect against *S. aureus*, a ten-fold higher concentration of these ions had to be used due to its lower sensitivity. Lower susceptibility of *S. aureus* bacteria was also observed in previous studies conducted for composites containing bioglasses enriched with ZnO [5]. The observed higher antibacterial activity of bioglasses with a finer particle size could be associated with their higher specific surface area, and also favor the formation of mechanical damage to the bacterial cell wall [15]. Bioglasses P5 I and P5 II also showed antibacterial activity, which can be explained by the release of calcium ions. According to Zhang [38], an increase in the pH of the environment as a result of the release of ions leads to a reduction in the number of microorganisms.

6. Conclusions

Five bioglasses were produced using the sol-gel method in the SiO_2-P_2O_5-CaO system. The chemical compositions of glasses were enriched with SrO which increased osteogenicity or ZnO which increased antibacterial activity. Bioglasses were obtained in the form of coarse-grained powders, in two particle sizes: I and II. The bioglasses were evaluated via TG-DTA, FTIR, SEM-EDS analyses before and after incubation in SBF solution. The concentration of Ca^{2+} ions released into deionized water confirmed that the particle size has a smaller impact on degradation than the microstructure of bioglass. In the SEM images taken incubation in the SBF solution, well-visible spherical forms and changes in the chemical composition in the EDS analyzes were observed on the surface of all the tested bioglasses. LDH and WST-1 tests on human osteoblasts hFOB1.19 confirmed that the tested bioglasses were non-cytotoxic. The obtained results also showed that the cytotoxicity of the tested bioglasses is more influenced by

the chemical composition than the particle size. The proliferation results of all tested bioglasses exceeded the threshold of 70%. The highest antibacterial activity was shown by bioglasses enriched with zinc. The observed reduction results indicate a higher sensitivity of *P. aeruginosa* bacteria compared to *S. aureus* to bactericidal agents present in contact with the tested bioglasses. In addition, Ca^{2+} ions released from bioglass can increase the pH of the environment, and thus also reduce the number of microorganisms. The improved methodology based on cell growth in cell culture inserts allowed for a better assessment of the effects of ion release on osteoblasts. The properties of the developed and produced bioglasses, including the results of physicochemical tests and *in vitro* biocompatibility assessment, allow them to be used in the further part of research on innovative multifunctional composites for filling bone defects.

Acknowledgments

This research was funded by NATIONAL CENTRE FOR RESEARCH AND DEVELOPMENT, Poland, grant number TECHMATSTRATEG 2/406384/7/NCBR/2019 (GlassPoPep - Multifunctional composite material with antimicrobial and pro-regenerative properties for the reconstruction of bone tissue).

References

[1] Baheiraei N, Eyni H, Bakhshi B, Najafloo R, Rabiee N. Effects of strontium ions with potential antibacterial activity on in vivo bone regeneration. Sci Rep 2021;11:1–9, DOI:10.1038/s41598-021-88058-1.

[2] Balasubramanian P, Strobel LA, Kneser U, Boccaccini AR. Zinc-containing bioactive glasses for bone regeneration, dental and orthopedic applications. Biomed Glas 2015;1:51–69, DOI:10.1515/bglass-2015-0006.

[3] Beyersmann D. Homeostasis and Cellular Functions of Zinc. Materwiss Werksttech 2002;33:764–9, DOI:10.1002/mawe.200290008.

[4] Cacciotti I. Bivalent cationic ions doped bioactive glasses: the influence of magnesium, zinc, strontium and copper on the physical and biological properties. J Mater Sci 2017;52:8812–31, DOI:10.1007/s10853-017-1010-0.

[5] Ciołek L, Biernat M, Jaegermann Z, Zaczyńska E, Czarny A, Jastrzębska A, et al. The studies of cytotoxicity and antibacterial activity of composites with ZnO-doped bioglass. Int J Appl Ceram Technol 2019;16:541–51, DOI:10.1111/ijac.13144.

[6] Deshmukh K, Kovářík T, Křenek T, Docheva D, Stich T, Pola J. Recent advances and future perspectives of sol-gel derived porous bioactive glasses: a review. RSC Adv 2020;10:33782–835, DOI:10.1039/d0ra04287k.

[7] El-Kady AM, Kamel NA, Elnashar MM, Farag MM. Production of bioactive glass/chitosan scaffolds by freeze-gelation for optimized vancomycin delivery: Effectiveness of glass presence on controlling the drug release kinetics. J Drug Deliv Sci Technol 2021;66:102779, DOI:10.1016/j.jddst.2021.102779.

[8] Fredholm YC, Karpukhina N, Brauer DS, Jones JR, Law R V., Hill RG. Influence of

strontium for calcium substitution in bioactive glasses on degradation, ion release and apatite formation. J R Soc Interface 2012;9:880–9, DOI:10.1098/rsif.2011.0387.

[9] Gentleman E, Fredholm YC, Jell G, Lotfibakhshaiesh N, O'Donnell MD, Hill RG, et al. The effects of strontium-substituted bioactive glasses on osteoblasts and osteoclasts in vitro. Biomaterials 2010;31:3949–56, DOI:10.1016/j.biomaterials.2010.01.121.

[10] Gerhardt LC, Boccaccini AR. Bioactive glass and glass-ceramic scaffolds for bone tissue engineering. Materials (Basel) 2010;3:3867–910, DOI:10.3390/ma3073867.

[11] Gorustovich AA, Steimetz T, Cabrini RL, Porto López JM. Osteoconductivity of strontium-doped bioactive glass particles: A histomorphometric study in rats. J Biomed Mater Res - Part A 2010;92:232–7, DOI:10.1002/jbm.a.32355.

[12] Hajduga MB, Bobiński R, Dutka M, Ulman-Włodarz I, Bujok J, Pająk C, et al. Analysis of the antibacterial properties of polycaprolactone modified with graphene, bioglass and zinc doped bioglass. Acta Bioeng Biomech 2021;23. https://doi.org/10.37190/ABB-01766-2020-03.

[13] Hench LL, Wheeler DL, Greenspan DC. Molecular Control of Bioactivity in Sol-Gel Glasses. J Sol-Gel Sci Technol 1998;13:245–50, DOI:10.1023/a:1008643303888.

[14] Hesaraki S, Gholami M, Vazehrad S, Shahrabi S. The effect of Sr concentration on bioactivity and biocompatibility of sol-gel derived glasses based on CaO-SrO-SiO2-P2O5 quaternary system. Mater Sci Eng C 2010;30:383–90, DOI:10.1016/j.msec.2009.12.001.

[15] Hu S, Chang J, Liu M, Ning C. Study on antibacterial effect of 45S5 Bioglass®. J Mater Sci Mater Med 2009;20:281–6, DOI:10.1007/s10856-008-3564-5.

[16] Isaac J, Nohra J, Lao J, Jallot E, Nedelec JM, Berdal A, et al. Effects of strontium-doped bioactive glass on the differentiation of cultured osteogenic cells. Eur Cells Mater 2011;21:130–43, DOI:10.22203/eCM.v021a11.

[17] Ito A, Kawamura H, Otsuka M, Ikeuchi M, Ohgushi H, Ishikawa K, et al. Zinc-releasing calcium phosphate for stimulating bone formation. Mater Sci Eng C 2002;22:21–5, DOI:10.1016/S0928-4931(02)00108-X.

[18] Kargozar S, Lotfibakhshaiesh N, Ai J, Mozafari M, Brouki Milan P, Hamzehlou S, et al. Strontium- and cobalt-substituted bioactive glasses seeded with human umbilical cord perivascular cells to promote bone regeneration via enhanced osteogenic and angiogenic activities. Acta Biomater 2017;58:502–14, DOI:10.1016/j.actbio.2017.06.021.

[19] Kargozar S, Montazerian M, Hamzehlou S, Kim HW, Baino F. Mesoporous bioactive glasses: Promising platforms for antibacterial strategies. Acta Biomater 2018;81:1–19, DOI:10.1016/j.actbio.2018.09.052.

[20] Liu X, Ding C, Chu PK. Mechanism of apatite formation on wollastonite coatings in simulated body fluids. Biomaterials 2004;25:1755–61, DOI:10.1016/j.biomaterials.2003.08.024.

[21] Lukito D, Xue JM, Wang J. In vitro bioactivity assessment of 70 (wt.)%SiO2–30 (wt.)%CaO bioactive glasses in simulated body fluid. Mater Lett 2005;59:3267–71, DOI:10.1016/j.matlet.2005.05.055.

[22] Łączka M, Cholewa-Kowalska K, Osyczka AM. Bioactivity and osteoinductivity of glasses and glassceramics and their material determinants. Ceram Int 2016;42:14313–25, DOI:10.1016/j.ceramint.2016.06.077.

[23] Mao L, Xia L, Chang J, Liu J, Jiang L, Wu C, et al. The synergistic effects of Sr and Si bioactive ions on osteogenesis, osteoclastogenesis and angiogenesis for osteoporotic bone regeneration. Acta Biomater 2017;61:217–32, DOI:10.1016/j.actbio.2017.08.015.

[24] Moghanian A, Firoozi S, Tahriri M. Characterization, in vitro bioactivity and biological studies of sol-gel synthesized SrO substituted 58S bioactive glass. Ceram Int 2017;43:14880–90, DOI:10.1016/j.ceramint.2017.08.004.

[25] Mulani MS, Kamble EE, Kumkar SN, Tawre MS, Pardesi KR. Emerging Strategies to Combat ESKAPE Pathogens in the Era of Antimicrobial Resistance: A Review. Front Microbiol 2019;10, DOI:10.3389/fmicb.2019.00539.

[26] Murphy S, Wren AW, Towler MR, Boyd D. The effect of ionic dissolution products of Ca–Sr–Na–Zn–Si bioactive glass on in vitro cytocompatibility. J Mater Sci Mater Med 2010;21:2827–34, DOI:10.1007/s10856-010-4139-9.

[27] O'Donnell MD, Candarlioglu PL, Miller CA, Gentleman E, Stevens MM. Materials characterisation and cytotoxic assessment of strontium-substituted bioactive glasses for bone regeneration. J Mater Chem 2010;20:8934, DOI:10.1039/c0jm01139h.

[28] Pasquet J, Chevalier Y, Pelletier J, Couval E, Bouvier D, Bolzinger MA. The contribution of zinc ions to the antimicrobial activity of zinc oxide. Colloids Surfaces A Physicochem Eng Asp 2014;457:263–74, DOI:10.1016/j.colsurfa.2014.05.057.

[29] Saino E, Grandi S, Quartarone E, Maliardi V, Galli D, Bloise N, et al. In vitro calcified matrix deposition by human osteoblasts onto a zinc-containing bioactive glass. Eur Cells Mater 2011;21:59–72, DOI:10.22203/eCM.v021a05.

[30] Saravanapavan P, Hench LL. Mesoporous calcium silicate glasses. I. Synthesis. J Non Cryst Solids 2003;318:1–13, DOI:10.1016/S0022-3093(02)01864-1.

[31] Sergi R, Bellucci D, Cannillo V. A review of bioactive glass/natural polymer composites: State of the art. Materials (Basel) 2020;13:1–38, DOI:10.3390/ma13235560.

[32] Silva BL da, Abuçafy MP, Manaia EB, Junior JAO, Chiari-Andréo BG, Pietro RCLR, et al. Relationship between structure and antimicrobial activity of zinc oxide nanoparticles: An overview. Int J Nanomedicine 2019;14:9395–410, DOI:10.2147/IJN.S216204.

[33] Strobel LA, Hild N, Mohn D, Stark WJ, Hoppe A, Gbureck U, et al. Novel strontium-doped bioactive glass nanoparticles enhance proliferation and osteogenic differentiation of human bone marrow stromal cells. J Nanoparticle Res 2013;15, DOI:10.1007/s11051-013-1780-5.

[34] Vaid C, Murugavel S, Das C, Asokan S. Mesoporous bioactive glass and glass-ceramics: Influence of the local structure on in vitro bioactivity. Microporous Mesoporous Mater 2014;186:46–56, DOI:10.1016/j.micromeso.2013.11.027.

[35] Vukomanovic M, Gazvoda L, Anicic N, Rubert M, Suvorov D, Müller R, et al. Multi-doped apatite: Strontium, magnesium, gallium and zinc ions synergistically affect osteogenic stimulation in human mesenchymal cells important for bone tissue

engineering. Biomater Adv 2022;140:213051, DOI:10.1016/j.bioadv.2022.213051.

[36] Wu C, Ramaswamy Y, Chang J, Woods J, Chen Y, Zreiqat H. The effect of Zn contents on phase composition, chemical stability and cellular bioactivity in Zn-Ca-Si system ceramics. J Biomed Mater Res - Part B Appl Biomater 2008;87:346–53, DOI:10.1002/jbm.b.31109.

[37] Yan M, Song Y, Wong CP, Hardin K, Ho E. Zinc deficiency alters DNA damage response genes in normal human prostate epithelial cells. J Nutr 2008;138:667–73, DOI:10.1093/jn/138.4.667.

[38] Zhang D, Hupa M, Hupa L. In situ pH within particle beds of bioactive glasses. Acta Biomater 2008;4:1498–505, DOI:10.1016/j.actbio.2008.04.007.

[39] Zheng K, Boccaccini AR. Sol-gel processing of bioactive glass nanoparticles: A review. Adv Colloid Interface Sci 2017;249:363–73, DOI:10.1016/j.cis.2017.03.008.

[40] Zheng K, Lu M, Rutkowski B, Dai X, Yang Y, Taccardi N, et al. ZnO quantum dots modified bioactive glass nanoparticles with pH-sensitive release of Zn ions, fluorescence, antibacterial and osteogenic properties. J Mater Chem B 2016;4:7936–49, DOI:10.1039/C6TB02053D.